2024 IEEE International Conference on Robotics and Automation (ICRA 2024)
May 13-17, 2024. Yokohama, Japan

Towards Robo-Coach: Robot Interactive Stiffness/Position Adaptation for Human Strength and Conditioning Training

Chenzui Li[1], Xi Wu[1], Tao Teng[1,2], Sylvain Calinon[3], and Fei Chen[1†]

***Abstract*— Traditional strength and conditioning training relies on the utilization of free weights, such as weighted implements, to elicit external stimuli. However, this approach poses a significant challenge when attempting to modify or adjust the loads within a single training set. This paper introduces an innovative method for achieving adjustable loads during resistance training by leveraging physical Human-Robot Interaction (pHRI). The primary objective is to regulate targeted muscle activation through the use of Robo-Coach (robotic coach system). We first utilize a Task-Parameterized Gaussian Mixture Model (TP-GMM) to learn the motion of coach demonstration, which can be generalized for the trainees. The 3D path extracted from the generated trajectory is then projected onto a 2D plane with respect to the direction of the load. Furthermore, we propose a hybrid stiffness/position generator for online task execution. This generator determines the desired positions in the 2D plane according to the contact point displacements in the stimuli direction and, simultaneously, sets the desired stiffness based on the muscle activation feedback. Finally, the Robo-Coach is implemented with a variable impedance controller to achieve load-adjustable resistance training with the trainee. The biceps curl exercises were conducted and the results showed favorable performance, indicating the effectiveness of this approach.**

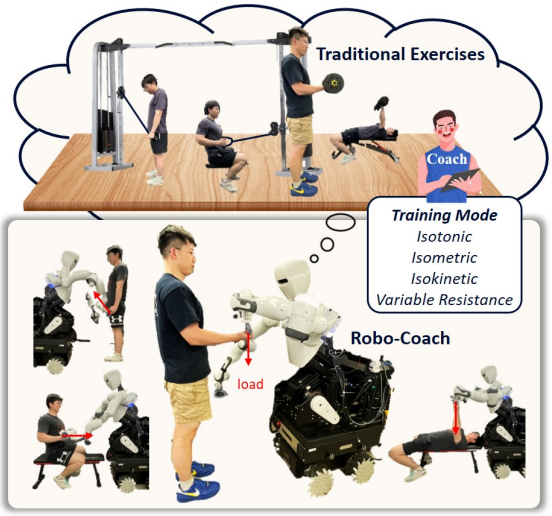

Fig. 1. Concept of Robo-Coach from the inspiration of traditional strength and conditioning training under the guidance of coaches. In this scenario, the robot can perform various exercises with trainees by adapting the loads to achieve different training modes.

I. INTRODUCTION

Traditional strength/resistance training uses free weights such as Olympic bars or weighted implements to provide external loads/stimulus [1]. However, offering trainees a greater variety of training modes during their resistance exercises can significantly enhance their strength improvements by increasing the ways of overloading the muscles [2]. Variable resistance training (VRT) is one of the training modes that vary the external resistance during one single repetition to maximize muscle strength [3] and has outperformed traditional resistance training in producing muscle gains during exercises such as bench press [4] and back squat [5]. To achieve this, elastic bands or iron chains are widely applied and added to alter loads at different phases of movement with growth of the average muscle activation compared to free-weighted one [6], [7]. Nevertheless, these assistive devices can only provide a feedforward training pattern during repetitions, in which the variation of resistance loads is non-adjustable.

A robotic system is able to produce VRT by directly interacting with the human trainee and providing real-time feedback to the robot. Consequently, the robot can dynamically adjust the training loads based on the trainee's requirements and conditions. Several robotic exercise machines have been developed by altering the training resistances to make trainees more effective in strength training [8], [9]. In [10], the authors developed a robotic biceps exercise system to measure and control the resistance force throughout the exercise range of motion, resulting in maximal muscular gain. In addition, assistive robot systems have been constructed for rehabilitation training of the range of motion and muscle strength [11], [12], which can be regarded as a type of muscle strength training. However, these robotic systems are mostly developed on the basis of traditional equipment, which can only perform limited types of exercises. Additionally, the above systems do not support real-time muscle-level control, which is supposed to be an essential part of resistance training [2]. Hence, a universal robot with the ability to directly interact with the trainees to perform proper motion and load for diverse exercises with real-time human muscle feedback can provide manifold exercises and training modes (such as the Robo-Coach in Fig. 1).

This work was supported in part by the Research Grants Council of the Hong Kong SAR under Grant 14211723, 14222722 and C7100-22GF and in part by InnoHK of the Government of Hong Kong via the Hong Kong Centre for Logistics Robotics.

[1]Chenzui Li, Xi Wu, Tao Teng and Fei Chen are with the Department of Mechanical and Automation Engineering, T-Stone Robotics Institute, The Chinese University of Hong Kong, Hong Kong (e-mail: czli@mae.cuhk.edu.hk, xwu@mae.cuhk.edu.hk, tao.teng@cuhk.edu.hk, f.chen@ieee.org).

[2] Tao Teng is also with the Hong Kong Center for Logistics Robotics, Hong Kong.

[3]Sylvain Calinon is with the Idiap Research Institute, Martigny, Switzerland (e-mail: sylvain.calinon@idiap.ch).

[†]Corresponding authors

The traditional approach owns advantages such as the rationality of the movement while doing free weight training under the guidance of coaches [1]. Hence, it makes sense to transfer those motion paths to robots. The Learning from Demonstration (LfD) method can teach a robot the paths/trajectories in Cartesian space, which include imitation learning approaches such as Dynamic Movement Primitives (DMP) [13] or Gaussian Mixture Model (GMM) [14], [15] which are widely used in human-robot interaction to represent complex human demonstration motions with few parameters that can be flexibly adjusted, and reinforcement learning approach such as various neural network models [16]. The extension of GMM, namely TP-GMM [17], trained using the expectation-maximization (EM) algorithm [18], can represent demonstration motion profiles from several different perspectives for integrating task information and has been applied in many interactive tasks like object lifting [19] and cucumber cutting [20]. This approach has the ability to generalize the motion paths to new situations, which is necessary for our resistance training tasks due to differences in body/personal parameters among different trainees.

On the other hand, to achieve adjustable external loads during the interaction with a trainee, impedance controllers can be used by tuning the parameters such as stiffness, damping, and inertia. However, how to tune the parameters according to human conditions is an open question. Electromyography (EMG) signals are the result of muscle bio-electrical activity. They reflect the operator's muscle voluntary contractions, providing insight into his muscle conditions, and thus are often used in the impedance control strategies of collaborative robotic systems. Muscle activation levels have been calculated by means of surface EMG to design the variable impedance controllers [21], [22]. A method is proposed that allows the robot to adapt its physical behavior to human muscle activation based on EMG feedback [23]. Authors propose a control strategy for the adaptation of the impedance of collaborative robots, based on the operator's intentions and movements, which are estimated using a real-time EMG to force model [24]. The above studies have verified the effectiveness of EMG-based human-robot interfaces.

In this paper, we propose a novel approach for physical human-robot interaction aimed at monitoring the muscle activation level of humans as they move along a learned path. To acquire the trajectory of a specific exercise, we use a TP-GMM to model the motion of expert demonstration, enabling generalization to new start and endpoints. We then developed a hybrid stiffness/position generator that determines the attractor points of the robot end effector and the corresponding stiffness based on the interactive process of resistance training between humans and robots. Note that the robot is supposed to passively track the trainee's motion while making adjustments to the motion path in the projection plane. Simultaneously, the external load is generated using a PD controller, where the stiffness values are fine-tuned based on the feedback received from muscle activation. Finally, the robot uses a variable impedance controller to interact with the trainee on the force level to achieve the task of EMG-based variable resistance training. The proposed approach was validated with experiments on a Collaborative dUal-arm Robot manIpulator (CURI). The biceps curl exercises are selected as the task.

In summary, the contributions of this work are concluded as follows:

- We propose a novel framework for implementing human strength and conditioning training by using physical human-robot interaction to replace the traditional resistance training approach which requires counterweights.
- A learning method to generate customized training paths for different trainees based on expert demonstrations is released to standardize training actions.
- An online EMG-based variable stiffness controller is proposed to achieve variable resistance training by monitoring and adjusting the target muscle activation for effective training.

II. PROPOSED METHODS

The diagram of the overall framework is illustrated in Fig. 2. Our proposed methods are shown in this section to combine the interaction model, imitation learning, and a hybrid position/stiffness generator for learning and generating human-robot interactive resistance training tasks.

A. Interaction Model and Robot Impedance Controller

During Human-Robot Interaction, the motion of the robot's end effector is produced by the collaborative effect of the robot control input $\boldsymbol{f}^r$ and the external force $\boldsymbol{f}^e$ from human, which can be represented as a unit mass moving in Cartesian space:

$$\ddot{\boldsymbol{p}} = \boldsymbol{f}^r + \boldsymbol{f}^e \tag{1}$$

where $\ddot{\boldsymbol{p}}$ is the acceleration of the unit mass in the world coordinates. We assume that $\boldsymbol{f}^r$ is powered by a virtual spring-damper system and (1) can be rewritten as:

$$\ddot{\boldsymbol{p}} = \boldsymbol{K}^d(\boldsymbol{p}^d - \boldsymbol{p}) + \boldsymbol{D}^d(\dot{\boldsymbol{p}}^{\boldsymbol{d}} - \dot{\boldsymbol{p}}) + \boldsymbol{f}^e \tag{2}$$

where $\boldsymbol{p}^d$ represent the position of the attractor, $\boldsymbol{K}^d$ and $\boldsymbol{D}^d$ are the stiffness and the damping diagonal matrices, respectively.

The interaction model provides us with a way to alter the robot's physical behavior during physical Human-Robot Interaction. Hence, we propose to achieve the desired dynamics by seeking the attractor point and the proper stiffness. Specifically, the variable $\boldsymbol{p}^d$ will be learned from human demonstration produced by the individual who is about to do resistance training with the robot. The virtual stiffness $\boldsymbol{K}^d$ is supposed to vary based on the task requirements. Note that the values in virtual damping $\boldsymbol{D}^d$ are predetermined as constant.

As mentioned above, we propose to learn the attractor values from traditional resistance training exercises. However, we can only observe the actual track $\boldsymbol{p}$ of the demonstrations instead of the variable $\boldsymbol{p}^d$. To address the aforementioned problem, we imagine the dumbbell as a 'robot' and assume that the movement of the 'robot' during the interaction with

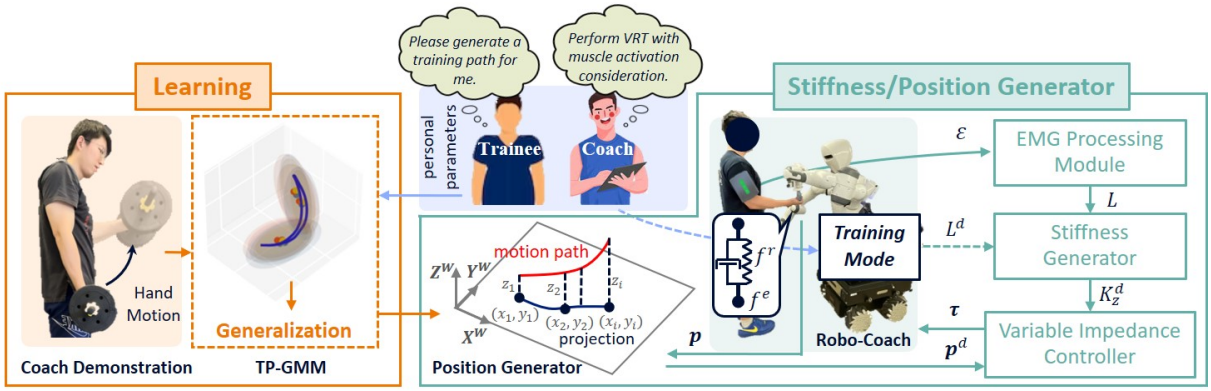

Fig. 2. The overall framework scheme. *Learning:* Coach/expert demonstrations of traditional resistance training are recorded and a TP-GMM is trained. *Hybrid Stiffness/Position Generator:* The personal parameters of a new trainee are given to generate a corresponding motion path. Using the real-time feedback of the robot end effector position, the desired attractor of the robot is obtained by referring to the given path. Simultaneously, the robot endpoint stiffness is calculated by a variable stiffness generator based on the real-time EMG feedback. Finally, given the desired stiffness and the attractor, a variable impedance controller is applied to drive the joint torques of the robot to achieve changeable loads during human-robot interaction.

the human is also a spring-damper system with the control input fixed (g in gravity direction). During the interaction, the human and the 'robot' share the same velocity and acceleration while there exists a constant displacement d between their positions in Z^w-axes with respect to the world coordinates. In other words, the control input g is generated by the virtual spring with a fixed stiffness K_z^g which satisfies $g = K_z^g d$. Hence, the dynamic model can be written by referring to (2):

$$\ddot{\boldsymbol{p}} = \boldsymbol{K}^g(\boldsymbol{p}^d - \boldsymbol{p}) + \boldsymbol{f}^e \tag{3}$$

where $\boldsymbol{K}^g$ represents the Cartesian stiffness matrix, $\boldsymbol{p}^d - \boldsymbol{p} = [0,0,d,0,0,0]^T$. Therefore, the variable $\boldsymbol{p}^d$ can be calculated accordingly.

The Cartesian impedance controller of our Robo-Coach, CURI, is then introduced to achieve human-robot interaction. CURI is a Dual-Arm mobile platform (as shown in Fig. 2). In this paper, we only apply one torque-controlled 7-DoF Franka Emika Panda robotic arm to achieve the tasks.

The dynamics of the robot can be written as [25]:

$$\boldsymbol{M}(\boldsymbol{q})\ddot{\boldsymbol{q}} + \boldsymbol{C}(\boldsymbol{q},\dot{\boldsymbol{q}})\dot{\boldsymbol{q}} + \boldsymbol{g}(\boldsymbol{q}) = \boldsymbol{\tau} + \boldsymbol{\tau}^e \tag{4}$$

where $\boldsymbol{q}$ represents the joint angles vector of the robotic arm, $\boldsymbol{M}(\boldsymbol{q})$ is the corresponding joint-space inertia matrix, $\boldsymbol{C}(\boldsymbol{q},\dot{\boldsymbol{q}})$ is the Coriolis/centrifugal matrix, and $\boldsymbol{g}(\boldsymbol{q})$ the vector of gravity. $\boldsymbol{\tau}$ and $\boldsymbol{\tau}^e = \boldsymbol{J}^T\boldsymbol{f}^e$ represent the corresponding control input and external torque in joint space, respectively. $\boldsymbol{J}$ is the robotic arm Jacobian matrix.

With the given robot dynamic (4) and interaction model (1), the reference joint torques $\boldsymbol{\tau}$ can be calculated. The Cartesian impedance controller proposed in [26] can be extended to CURI, while its stability can also be guaranteed.

$$\boldsymbol{\tau} = \boldsymbol{\tau}^{task} + \boldsymbol{\tau}^{null} \tag{5}$$

The $\boldsymbol{\tau}^{task}$ corresponding to the given main task is:

$$\boldsymbol{\tau}^{task} = \boldsymbol{J}^T(-\boldsymbol{K}^d(\boldsymbol{p} - \boldsymbol{p}^d) - \boldsymbol{D}^d(\dot{\boldsymbol{p}} - \dot{\boldsymbol{p}}^d)) \tag{6}$$

The null-space task input is defined as:

$$\boldsymbol{\tau}^{null} = (\boldsymbol{I} - \boldsymbol{J}^T\boldsymbol{J}^{+T})\boldsymbol{\tau}^0 \tag{7}$$

where $\boldsymbol{\tau}^0$ represents the corresponding torque projected in the null space of the main task, $\boldsymbol{N}(\boldsymbol{q}) = \boldsymbol{I} - \boldsymbol{J}^T\boldsymbol{J}^{+T}$ is the projection matrix in order to prevent interference with the Cartesian impedance behavior of the main task according to [27]. $\boldsymbol{J}^+$ expresses the generalized inverse of $\boldsymbol{J}$.

Finally, $\boldsymbol{\tau}$ is sent to the robotic arm directly through its torque command interface.

B. Learning

In traditional resistance training, the motion path of each trainee with respect to the world coordinates is different from the other when doing the same exercises due to differences in body size. In this paper, we propose to learn the motion from demonstrations by observing the experienced trainee/coach perform resistance training with dumbbells or weighted implements, which can be further applied to scale the reference path for other individuals such as fitness rookies based on their characteristics.

A TP-GMM model is adopted to inspect the demonstrations from different coordinates. More specifically, GMMs cluster points on the demonstration into multiple Gaussian distributions in each frame $j \in [1,P]$ and a motion considered the task parameter can be reproduced via the product of experts (PoE) [17]. The task parameter refers to the pose of the target object or the state of the environment, which depends on the specific task. In this paper, the task/personal parameter is the transformation matrices of the start point and endpoint of multiple demonstrations $\boldsymbol{\zeta}$ from the world origin, namely $\{\boldsymbol{b}^{(j)}, \boldsymbol{A}^{(j)}\}_{j=1,2}$. We first use these matrices to transform and align demonstrations with respect to each observer frame $\boldsymbol{X}_t^{(j)} = \boldsymbol{A}^{(j)^{-1}}(\boldsymbol{\zeta}_t - \boldsymbol{b}^{(j)})$. Then we use a TP-GMM with N Gaussian distributions $\{\boldsymbol{\mu}_k^{(j)}, \boldsymbol{\Sigma}_k^{(j)}\}_{j=1,2}, k \in [1,N]$ to represent $\boldsymbol{X}_t^{(j)}$ in each frame. Thus, the reproduction is expected to lie within the distributions $\mathcal{N}\left(\hat{\boldsymbol{\xi}}_k^{(j)}, \hat{\boldsymbol{\Sigma}}_k^{(j)}\right)_{j=1,2}$,

where $\hat{\boldsymbol{\xi}}_k^{(j)} = \boldsymbol{A}^{(j)}\boldsymbol{\mu}_k^{(j)} + \boldsymbol{b}^{(j)}$, $\hat{\boldsymbol{\Sigma}}_k^{(j)} = \boldsymbol{A}^{(j)}\boldsymbol{\Sigma}_k^{(j)}\boldsymbol{A}^{(j)^\top}$.

To reproduce the motion under new circumstances for generalization purposes, the transformation matrices of the start point and endpoint are changed to adapt to a new subject, and a new GMM is generated by PoE:

$$\mathcal{N}\left(\hat{\boldsymbol{\xi}}_k, \hat{\boldsymbol{\Sigma}}_k\right) \propto \prod_{j=1}^{2} \mathcal{N}\left(\hat{\boldsymbol{\xi}}_k^{(j)}, \hat{\boldsymbol{\Sigma}}_k^{(j)}\right) \tag{8}$$

with the result as $\hat{\boldsymbol{\Sigma}}_k = \left(\sum_{j=1}^{P} \hat{\boldsymbol{\Sigma}}_k^{(j)^{-1}}\right)^{-1}$, $\hat{\boldsymbol{\xi}}_k = \hat{\boldsymbol{\Sigma}}_k \sum_{j=1}^{P} \hat{\boldsymbol{\Sigma}}_k^{(j)^{-1}} \hat{\boldsymbol{\xi}}_k^{(j)}$. Thus, the reproduced motion $\hat{\boldsymbol{\zeta}}$ from this GMM should follow the style of demonstrations and start and end to fit the new trainee.

C. Hybrid Stiffness/Position Generator

On the one hand, we propose to produce the attractor $\boldsymbol{p}^d$ based on the robot state feedback in Cartesian space. After generating the motion $\hat{\boldsymbol{\zeta}}$ from section II-B, we obtain a path for the robot to track in the world coordinates and decompose it up by projection in the Z^w direction, which is shown in Fig. 2. Hence, we have a corresponding point (x_i, y_i) for each z_i in X^wY^w plane. The reason we handle the path in this way is because we expect the robot to give the trainee loads along the Z^w direction while tracking the path in the X^wY^w plane. The combination of path tracking and compliant movement for robots in different directions has been proven to be effective in rehabilitation scenarios [28], [29], which is highly relevant to resistance training. During the physical human-robot interaction, the human trainee is supposed to flex the elbow joint and generate external force to lift the robot end effector. By getting the position information $\boldsymbol{p}$ from the robot Cartesian state feedback, the attractor variables x^d, y^d in X^wY^w plane can be searched while the variable z^d can be calculated with the displacement d. Finally, the attractor $\boldsymbol{p}^d$ is given as the input of the impedance controller of CURI robot and it will passively follow the reference path. Note that the orientation is fixed.

On the other hand, we expect to realize one specific training mode by changing the stiffness of the variable impedance controller. Since traditional exercises are not defined in terms of muscle activation, we apply the variable resistance training mode with muscle fatigue consideration to vary the stiffness in this paper. More specifically, the trainees are trained by monitoring muscle activation and maintaining it at a desired level. Electromyography (EMG) is able to scrutinize muscle activity and the innervated nerve cells. Hence, we utilize the EMG signals as feedback to vary the stiffness value in Z axes, which will further increase/decrease the robot control input. We filter and rectify the raw EMG signals and then normalise the processed data ε by using maximal voluntary contraction (MVC) ε_{mvc}. The activation level of the muscle L is given:

$$L = \frac{\varepsilon}{\varepsilon_{mvc}} \in [0, 1] \tag{9}$$

To achieve monitorable and controllable resistance training at the muscle level, our approach changes the load force by adjusting stiffness online and achieves control effects by indirectly affecting the muscle activation level. Note that $\boldsymbol{K}^d = diag(K_x^d, K_y^d, K_z^d, K_\alpha^d, K_\beta^d, K_\gamma^d)$. With the reference muscle activation L^d, a PD controller is applied to tune the stiffness value K_z^d, which can be written as:

$$K_z^d = \lambda\left(k^p(L^d - L) + k^d(\dot{L}^d - \dot{L})\right) \tag{10}$$

where k^p and k^d represent the proportional gain and the derivative gain of PD controller, respectively. λ represents the scaling factor.

III. EXPERIMENTS

Experiments were conducted with 3 subjects including one senior trainee with seven years of fitness experience and two junior trainees who started strength training no more than two years. The age averaged 25 ± 3 years old while the body height averaged 1.83 ± 0.04 m. Note that the senior is regarded as the coach while the juniors are the trainees in this paper.

A. Data Collection and Processing

During the data collection process, the data of the dumbbell biceps curl exercises were recorded by the Optitrack system and EMG sensors with the corresponding software. The senior trainee's motion was obtained from the marker of the Optitrack system on the right hand to record its motion at a frequency of 100 Hz. The data were used for offline learning to generate a proper representation of the robot's motion path. Besides, the demonstrator was wearing the EMG sensor on the biceps brachii to record the muscle activities. Note that the placement of the EMG sensor is guided by the SENIAM recommendations [30]. The EMG signals were acquired through the Delsys Trigno Wireless System with a sampling rate of 2000 Hz.

We utilized three trajectories of coach demonstrations in GMM to represent biceps curl exercise motion. The result of the representation with regard to the PoE was illustrated for the human-robot interactive task in Fig. 2. Furthermore, by adding the task parameter and extending to TP-GMM, the motion reproduction was achieved with the initial and final locations of the end effector and one generated motion path was extracted. Full-wave rectification and a low-pass third-order Butterworth filter at 6 Hz are applied to the raw EMG signals, and the result was normalized according to MVC.

It is worth noting that the collection and preprocessing of the multimodal demonstration data such as optical and EMG signals, and the implementation of the TP-GMM method depend on the Rofunc package, a full-process python package for robot learning from demonstration published by our lab [31]. It provides numerous interfaces for demonstration collection and processing, baseline LfD methods, planning methods, and Isaac Gym-based simulators. At the same time, the method of recording hand movements based solely on vision is also applicable in low-cost situations [32], [33].

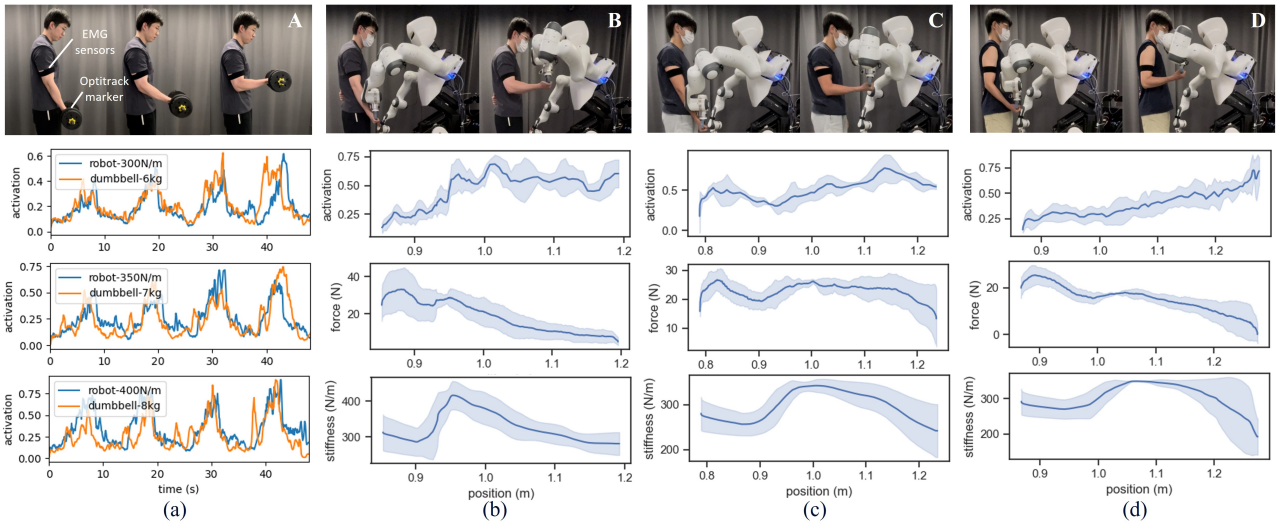

Fig. 3. The snapshots of experiments. *A:* senior demonstration of traditional dumbbell biceps curls with isotonic training, *B:* reproduction by the robot and interaction with senior under EMG-based VRT, *C & D:* generalization of motion paths to two juniors with variable resistance of the robot. The experimental results. *(a):* comparison of the biceps brachii muscle activation level of the senior between the robotic and traditional exercises under isotonic training, *(b) & (c) & (d):* change curves of muscle activation, interactive force, and stiffness in the load direction of three subjects with the same reference muscle activation value (0.5). Shaded areas represent the standard deviation estimated from the results of 4 repetitions.

TABLE I

AVERAGE MUSCLE ACTIVATION AND INTERACTIVE FORCE DURING HUMAN-ROBOT INTERACTION

	Average Muscle Activation				**Average Interactive Force (N)**			
Subject	**Isotonic Training**			**EMG-based VRT**	**Isotonic Training**			**EMG-based VRT**
Label	***Low***	***Middle***	***High***		***Low***	***Middle***	***High***	
Senior	0.24 ± 0.12	0.34 ± 0.15	0.51 ± 0.18	0.43 ± 0.18	23.2 ± 9.6	27.6 ± 9.8	33.3 ± 10.1	21.5 ± 10.3
Junior 1	0.41 ± 0.18	0.41 ± 0.16	0.52 ± 0.23	0.48 ± 0.16	14.9 ± 4.5	30.1 ± 9.3	32.7 ± 7.7	23.8 ± 4.7
Junior 2	0.15 ± 0.06	0.31 ± 0.17	0.42 ± 0.14	0.42 ± 0.17	14.0 ± 10.2	15.8 ± 14.0	18.4 ± 14.4	14.8 ± 7.4

B. Interaction with isotonic training mode

Firstly, we reproduced the isotonic mode of biceps resistance training with dumbbells through the movement generated by the interaction between the robot and the senior trainee. With the virtual displacement $d = 0.2\ m$, three constant stiffness values in the Z direction ($K_z^d = 300, 350, 400\ N/m$) with respect to the world frame were given for the robot to conduct different loads of biceps curl exercises. The stiffness values in the other two directions were set as $K_x^d, K_y^d = 300\ N/m$. The rotational stiffness values were set as $40\ Nm/rad$. The damping was not considered in this task since we only focused on tracking the path. The frequency of the impedance controller of our CURI robot is 1000 Hz. The EMG signals of the biceps muscle were recorded and processed at a frequency of 10 Hz. Note that the trainee got 10 minutes to rest between two training sets.

The snapshots of human demonstrations and human-robot interaction of biceps curl were shown in Fig. 3. With the trajectories collected from senior demonstrations (A), the robot reproduced the movement by interacting with the senior under constant stiffness values. The comparison of the biceps brachii activation levels between the dumbbell and robot exercises under different weights/loads was given in Fig. 3(a). It was shown that the trends and the amplitudes in muscle activation of the two types of exercises were similar. They both increase with the rise in height at the beginning of the path and then decrease after reaching a peak. Besides, the overall muscle activation was detected to be higher while the stiffness value was increased, which showed the same phenomenon as adding weights during traditional exercises. Hence, our proposed approach can provide a similar resistance training compared to the traditional one.

We then generated the new motion paths for the junior trainees based on their personal parameters, which contain the new start and ending locations. These two poses were collected directly on the robot by setting the robot to Kinesthetic teaching mode. After that, the two junior trainees conducted 4 repetitions of the biceps curl exercises with isotonic mode. The parameters were set to the same as when the senior trained while the stiffness values decreased to 200, 250, and 300 N/m for the juniors. The average biceps muscle activities of both junior trainees and the average interactive forces were calculated and shown in Table I. It was shown that, with the growth of stiffness, the average muscle activation and average interactive force gradually increased, which showed the same trend as the senior (from 0.24 ± 0.12 to 0.51 ± 0.18 and from $23.2 \pm 9.6\ N$ to $33.3 \pm 10.1\ N$). The difference in the growth margin is mainly caused by the muscle conditions.

According to the similar trends of muscle activation and interactive force between the senior and juniors, the conclusion that the robot can achieve the same training effect as the dumbbell training in activation level can be drawn.

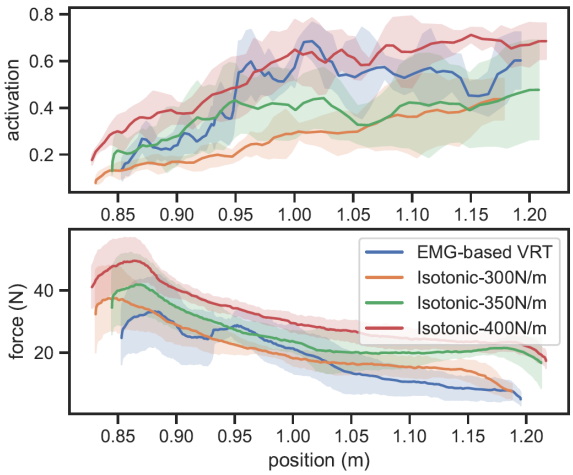

Fig. 4. Comparison of the muscle activation and the interactive forces between isotonic training and EMG-based VRT by the senior.

C. Interaction with EMG-based VRT mode

One of the advantages of Robo-Coach over traditional weighted implements is that the load can be changeable. Hence, we carried out the experiment of variable stiffness control based on EMG according to the aforementioned framework. More specifically, the stiffness generator based on a PD controller was applied to monitor and tune the muscle activation during human-robot interactive resistance training, which is supposed to prevent muscle fatigue. Giving the target muscle activation for our senior trainee, the PD controller was switched on to update the stiffness value K_z^d based on the real-time EMG feedback of the biceps brachii muscle. The minimum and maximum values of stiffness were set to 200 N/m and 450 N/m, respectively. The gains of PD controller k^p, k^d, and λ were set as 2.0, 0.1, and 50, respectively. The update frequency of the PD controller was 10 Hz. We first validated it on the senior trainee with the reference muscle activation value of 0.5.

The changing of corresponding muscle activation, interactive force, and stiffness value of the senior trainee with the positions of Z^w-axes were shown in Fig. 3(b). Note that only the concentric phase of biceps curls was given and 4 repetitions were conducted. It can be seen that when muscle activation was low at the beginning of each repetition, the stiffness value was growing and the interactive force was increasing accordingly. When muscle activation was detected over the reference activation level, the stiffness value dropped rapidly to decrease the interactive force and reduce muscle activation. The results showed that the senior's muscle activation oscillated around the expected value during the second half. In traditional training with heavy weights, trainees are likely to feel muscle fatigue and need assistance to complete the last few repetitions of one set. With our proposed framework, the muscle activation level of the target muscle is always under-monitored and can be tuned by varying stiffness.

Besides, the human-robot interaction with variable resistance was conducted by both junior trainees. One reference muscle activation level (0.5) was given for each individual and 4 repetitions were done by each junior. The results were illustrated in Fig. 3(c) and Fig. 3(d), respectively. Before testing, they both had experienced the EMG-based VRT mode on the Robo-Coach. The muscle activation results of both juniors were not as good as the senior trainee. It might be due to the fact that they did not control the lifting speed during the changing of external loads, which may cause abnormal changes in muscle activation. Hence, it will be essential for the trainee to control changes in training speed so that the jumps in muscle activation can be avoided.

D. Comparison between two training modes

Finally, we compared the variation of muscle activation levels and the interactive forces with two different modes by the senior trainee, which was shown in Fig. 4. From the perspective of muscle activities, the activation level grew steadily with height under isotonic mode while it increased rapidly to the reference value at the beginning and maintained under variable resistance. The changing curves of interaction forces under EMG-based VRT were also compared with isotonic mode, which demonstrates variations in interactive forces due to adjustments of stiffness. We also calculated and compared the average muscle activation and the average interactive force in Table I. It can be seen that the average interactive force during VRT mode (21.5 ± 10.3 N) was significantly lower than the value under isotonic mode (27.6 ± 9.8 N) while the average muscle activation under VRT mode (0.43 ± 0.18) was at the same level or even higher than isotonic mode (0.34 ± 0.15). In summary, the EMG-based VRT can activate the muscle faster and control the activation level within the range expected by the coach, which provides a technical foundation for muscle-oriented resistance training by human-robot interaction.

IV. CONCLUSIONS

In this paper, biceps curl exercises were achieved with isotonic mode and EMG-based VRT mode by physical human-robot interaction. Observing the motion of the coach demonstrations, a TP-GMM can be constructed to describe the reference motion of the specific resistance training exercise. This model can generate new motion paths for other trainees by applying their task/personal parameters. Then the robot can perform interactive resistance training with the trainee based on the corresponding path by an impedance controller. Besides, our approach can also change the input by tuning the stiffness value based on the muscle activation feedback. The experimental results successfully validate our methods with three subjects.

We provide an interface that can control the muscle activation during one single set of resistance training, so as to meet the demands of coaches/trainees at the muscle level. In the future, we expect to use a whole-body impedance controller for the humanoid robot to interact with trainees to generate greater loads and perform more types of resistance training such as bench press while ensuring human safety.

REFERENCES

[1] S. Schwanbeck, P. D. Chilibeck, and G. Binsted, "A comparison of free weight squat to smith machine squat using electromyography," *The Journal of Strength & Conditioning Research*, vol. 23, no. 9, pp. 2588–2591, 2009.

[2] T. J. Suchomel, S. Nimphius, C. R. Bellon, and M. H. Stone, "The importance of muscular strength: training considerations," *Sports medicine*, vol. 48, pp. 765–785, 2018.

[3] S. J. Fleck and W. Kraemer, *Designing resistance training programs, 4E*. Human Kinetics, 2014.

[4] M. A. Soria-Gila, I. J. Chirosa, I. J. Bautista, S. Baena, and L. J. Chirosa, "Effects of variable resistance training on maximal strength: A meta-analysis," *The Journal of Strength & Conditioning Research*, vol. 29, no. 11, pp. 3260–3270, 2015.

[5] M. A. Israetel, J. M. McBride, J. L. Nuzzo, J. W. Skinner, and A. M. Dayne, "Kinetic and kinematic differences between squats performed with and without elastic bands," *The Journal of Strength & Conditioning Research*, vol. 24, no. 1, pp. 190–194, 2010.

[6] B. J. Wallace, J. B. Winchester, and M. R. McGuigan, "Effects of elastic bands on force and power characteristics during the back squat exercise," *The Journal of Strength & Conditioning Research*, vol. 20, no. 2, pp. 268–272, 2006.

[7] A. H. Saeterbakken, V. Andersen, and R. Van den Tillaar, "Comparison of kinematics and muscle activation in free-weight back squat with and without elastic bands," *The Journal of Strength & Conditioning Research*, vol. 30, no. 4, pp. 945–952, 2016.

[8] C. Helland, E. Hole, E. Iversen, M. C. Olsson, O. R. Seynnes, P. A. Solberg, and G. Paulsen, "Training strategies to improve muscle power: is olympic-style weightlifting relevant?," *Medicine & Science in Sports & Exercise*, vol. 49, pp. 736–745, 2017.

[9] S. N. Cubero, G. Wirth, P. Kneale, and B. Nardi, "A mechatronic spotting system that mimics human weight-training assistance behavior," *Int. J. on Embedded Systems*, vol. 2, 2015.

[10] K. Kim and D. Hong, "Robotic biceps exercise machine: Hardware using series elastic actuator and control with disturbance observer," *IEEE Access*, vol. 8, pp. 12758–12767, 2019.

[11] M. Dong, W. Fan, J. Li, X. Zhou, X. Rong, Y. Kong, and Y. Zhou, "A new ankle robotic system enabling whole-stage compliance rehabilitation training," *IEEE/ASME transactions on mechatronics*, vol. 26, no. 3, pp. 1490–1500, 2020.

[12] G. Xu, X. Gao, S. Chen, Q. Wang, B. Zhu, and J. Li, "A novel approach for robot-assisted upper-limb rehabilitation: progressive resistance training as a paradigm," *International Journal of Advanced Robotic Systems*, vol. 14, no. 6, p. 1729881417736670, 2017.

[13] J. Liu, Y. Chen, Z. Dong, S. Wang, S. Calinon, M. Li, and F. Chen, "Robot cooking with stir-fry: Bimanual non-prehensile manipulation of semi-fluid objects," *IEEE Robotics and Automation Letters*, vol. 7, no. 2, pp. 5159–5166, 2022.

[14] S. Calinon and D. Lee, "Learning control," in *Humanoid Robotics: a Reference* (P. Vadakkepat and A. Goswami, eds.), pp. 1261–1312, Springer, 2019.

[15] Y. Gong, W. Tang, L. Zhou, L. Yu, and G. Qiu, "A discrete scheme for computing image's weighted gaussian curvature," in *2021 IEEE International Conference on Image Processing (ICIP)*, pp. 1919–1923, IEEE, 2021.

[16] Z. Dong, Z. Li, Y. Yan, S. Calinon, and F. Chen, "Passive bimanual skills learning from demonstration with motion graph attention networks," *IEEE Robotics and Automation Letters*, vol. 7, no. 2, pp. 4917–4923, 2022.

[17] S. Calinon, "A tutorial on task-parameterized movement learning and retrieval," *Intelligent service robotics*, vol. 9, no. 1, pp. 1–29, 2016.

[18] W. Zhao, S. Wang, Z. Xie, J. Shi, and C. Xu, "Gan-em: Gan based em learning framework," in *Proceedings of the Twenty-Eighth International Joint Conference on Artificial Intelligence, IJCAI-19*, pp. 4404–4411, International Joint Conferences on Artificial Intelligence Organization, 7 2019.

[19] L. Rozo, S. Calinon, D. G. Caldwell, P. Jimenez, and C. Torras, "Learning physical collaborative robot behaviors from human demonstrations," *IEEE Transactions on Robotics*, vol. 32, no. 3, pp. 513–527, 2016.

[20] C. Yang, C. Zeng, Y. Cong, N. Wang, and M. Wang, "A learning framework of adaptive manipulative skills from human to robot," *IEEE Transactions on Industrial Informatics*, vol. 15, no. 2, pp. 1153–1161, 2018.

[21] S. Grafakos, F. Dimeas, and N. Aspragathos, "Variable admittance control in phri using emg-based arm muscles co-activation," in *2016 IEEE International Conference on Systems, Man, and Cybernetics (SMC)*, pp. 001900–001905, IEEE, 2016.

[22] J. DelPreto and D. Rus, "Sharing the load: Human-robot team lifting using muscle activity," in *2019 international conference on robotics and automation (ICRA)*, pp. 7906–7912, IEEE, 2019.

[23] L. Peternel, N. Tsagarakis, D. Caldwell, and A. Ajoudani, "Adaptation of robot physical behaviour to human fatigue in human-robot co-manipulation," in *2016 IEEE-RAS 16th International Conference on Humanoid Robots (Humanoids)*, pp. 489–494, IEEE, 2016.

[24] M. Bednarczyk, H. Omran, and B. Bayle, "Emg-based variable impedance control with passivity guarantees for collaborative robotics," *IEEE Robotics and Automation Letters*, vol. 7, no. 2, pp. 4307–4312, 2022.

[25] R. Featherstone and D. Orin, "Robot dynamics: equations and algorithms," in *Proceedings 2000 ICRA. Millennium Conference. IEEE International Conference on Robotics and Automation. Symposia Proceedings (Cat. No. 00CH37065)*, vol. 1, pp. 826–834, IEEE, 2000.

[26] C. Ott, *Cartesian impedance control of redundant and flexible-joint robots*. Springer, 2008.

[27] O. Khatib, "A unified approach for motion and force control of robot manipulators: The operational space formulation," *IEEE Journal on Robotics and Automation*, vol. 3, no. 1, pp. 43–53, 1987.

[28] M. H. Barri, A. Widyotriatmo, *et al.*, "Path reference generation for upper-limb rehabilitation with kinematic model," in *2018 IEEE International Conference on Robotics, Biomimetics, and Intelligent Computational Systems (Robionetics)*, pp. 38–43, IEEE, 2018.

[29] Y. Zhao, C. Liang, Z. Gu, Y. Zheng, and Q. Wu, "A new design scheme for intelligent upper limb rehabilitation training robot," *International journal of environmental research and public health*, vol. 17, no. 8, p. 2948, 2020.

[30] H. J. Hermens, B. Freriks, C. Disselhorst-Klug, and G. Rau, "Development of recommendations for semg sensors and sensor placement procedures," *Journal of electromyography and Kinesiology*, vol. 10, no. 5, pp. 361–374, 2000.

[31] J. Liu, C. Li, D. Delehelle, Z. Li, and F. Chen, "Rofunc: The full process python package for robot learning from demonstration and robot manipulation," June 2023.

[32] Z. Xie, S. Wang, W. Zhao, and Z. Guo, "Context attention module for human hand detection," in *2019 IEEE International Conference on Multimedia & Expo Workshops (ICMEW)*, pp. 555–560, IEEE, 2019.

[33] Z. Xie, S. Wang, W. Zhao, and Z. Guo, "A robust context attention network for human hand detection," *Expert Systems with Applications*, vol. 208, p. 118132, 2022.